Inorganic Chemistry

Article

pubs.acs.org/IC

From Order to Disorder and Back Again: In Situ Hydrothermal Redox Reactions of Uranium Phosphites and Phosphates

Eric M. Villa,[†,‡] Connor J. Marr,[‡] Juan Diwu,[‡] Evgeny V. Alekseev,*[,§,∥] Wulf Depmeier,[⊥] and Thomas E. Albrecht-Schmitt*[,†,‡]

[†]Department of Chemistry and Biochemistry, Florida State University, 102 Varsity Way, Tallahassee, Florida 32306-4390, United States

[‡]Department of Civil Engineering and Geological Sciences and Department of Chemistry and Biochemistry, University of Notre Dame, 156 Fitzpatrick Hall, Notre Dame, Indiana 46556, United States

[§]Forschungszentrum Jülich GmbH, Institute for Energy and Climate Research (IEK-6), 52428, Jülich, Germany

[∥]Institut für Kristallographie, RWTH Aachen University, 52066 Aachen, Germany

[⊥]Institut für Geowissenschaften, Universität zu Kiel, Ludevig-Meyn Str. 10, 24118, Kiel, Germany

Supporting Information

ABSTRACT: Five new uranium phosphites, phosphates, and mixed phosphate−phosphite compounds were hydrothermally synthesized using H_3PO_3 as an initial reagent. These compounds are $Cs_4[(UO_2)_8(HPO_4)_5(HPO_3)_5]\cdot 4H_2O$ (**1**), $Cs[U^{IV}(PO_4)(H_{1.5}PO_4)]_2$ (**2**), $Cs_4[U^{IV}_6(PO_4)_8(HPO_4)(HPO_3)]$ (**3**), $Cs_{10}[U^{IV}_{10}(PO_4)_4(HPO_4)_{14}(HPO_3)_5]\cdot H_2O$ (**4**), and $Cs_3[U^{IV}_4(PO_4)_3(HPO_4)_5]$ (**5**). The first contains uranium(VI) and the latter four uranium(IV). Of the U^{IV} structures, two have extensive disordering among the cesium cation positions, one of which also contains disordering at some of the phosphate−phosphite positions. These intermediate compounds are bookended by nondisordered phases. The isolation of these transitional phases occurred at the higher of the pH conditions attempted here. Both the starting pH and the duration of the reactions have a strong influence on the products formed. Herein, we explore the second series of in situ hydrothermal redox reactions of uranyl nitrate with phosphorous acid and cesium carbonate. The isolation of these disordered crystalline products helps to illuminate the complex reaction pathways that can occur in hydrothermal syntheses.

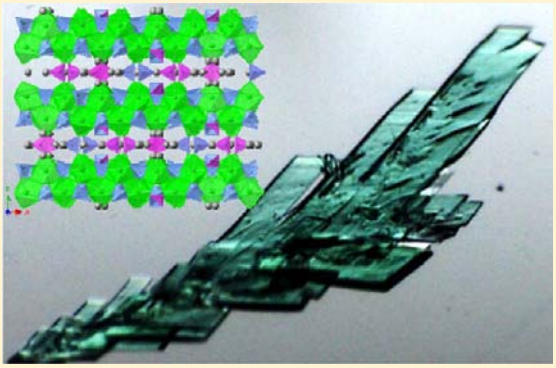

INTRODUCTION

Understanding the transportation of actinides through the environment is vital to our understanding of both natural deposits and the geological repositories where nuclear waste is, or could potentially be, stored. The naturally occurring isotopes of uranium are not as great of a radiation hazard as many of the other actinides, but uranium does pose problems in terms of the vast quantities used in the nuclear industry. Phosphate compounds may help to diminish the transport of some actinides owing to the generally low solubility of actinide phosphates, which has led to studies on their use as possible long-term storage materials.[1−7]

Phosphite, HPO_3^{2-}, has a tetrahedral geometry, and the phosphorus center is bound by three oxygen atoms and one hydrogen atom. Phosphite itself can be used as a precursor to making phosphonates, and many actinide phosphonates have been recently synthesized.[8] In phosphite, the phosphorus is P^{III} instead of the normal P^{V}, as in phosphate, which provides the opportunity for redox chemistry to take place. Unlike many other C_{3v} oxoanions, such as selenite, or tellurite, or iodate,[9−11] the phosphite anion is a strong reducing agent and helps to stabilize lower oxidation states for actinides. Here, the reduction potential at standard temperature and pressure for the reaction of $H_3PO_4 + 2H^+ + 2e^- \leftrightarrow H_3PO_3 + H_2O$ is −0.276. This reduction step is potentially useful because it could provide another way to limit the solubility of the products formed owing to the generally lower solubility of U^{IV} versus U^{VI}.

Actinide phosphites, in general, are underexplored, but several compounds with atypical structures have been prepared through the application of organic templates.[12−18] We have published on some simple actinide(IV) phosphites that demonstrated the actinide contraction across the series and the influence of the starting oxidation state of the actinide used on product composition.[19] Here, the phosphite anion helped to stabilize the lower oxidation states of other actinides with multiple stable oxidation states, such as neptunium and plutonium, with potential waste storage implications. Additionally, we have recently reported on a series of compounds that

Received: October 9, 2012
Published: January 9, 2013

   dx.doi.org/10.1021/ic302198w | Inorg. Chem. 2013, 52, 965−973

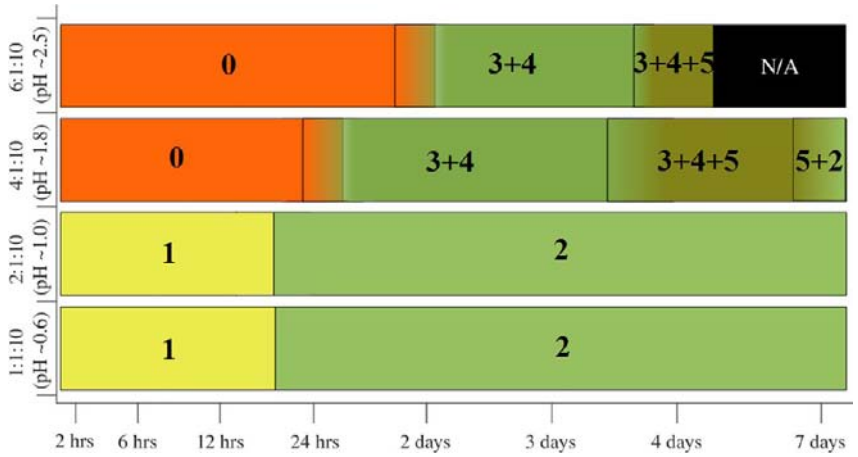

Figure 1. Products that form as a function of time and the ratio of reactants in a cesium carbonate–uranyl nitrate–phosphorous acid system, which contains a 10:1 ratio of H_3PO_3:UO_2^{2+} with varying Cs_2CO_3 concentrations. Time is on the *x* axis, and the reactant ratios on the *y* axis are Cs_2CO_3:UO_2^{2+}:H_3PO_3. Here, the products shown are **0**, $Cs_2[(UO_2)_2(HPO_3)_3]\cdot H_2O$; **1**, $Cs_4[(UO_2)_8(HPO_4)_5(HPO_3)_5]\cdot 4H_2O$; **2**, $Cs[U^{IV}(PO_4)(H_{1.5}PO_4)]_2$; **3**, $Cs_4[U^{IV}_6(PO_4)_8(HPO_4)(HPO_3)]$; **4**, $Cs_{10}[U^{IV}_{10}(PO_4)_4(HPO_4)_{14}(HPO_3)_5]\cdot H_2O$; and **5**, $Cs_3[U^{IV}_4(PO_4)_3(HPO_4)_5]$. All products save (**0**) are new.[20] The overlapping colors, boxes, and addition signs indicate mixtures of compounds. Also, reactions were sampled at each point listed on the *x* axis.

explored the in situ redox chemistry that plays out in the uranium–phosphite system.[20] Here, we found that the starting pH and reaction duration were key in the formation of new products and, more importantly, we were able to isolate two transitional $U^{VI/IV}$ mixed phosphate–phosphite compounds.

Uranium has two readily accessible oxidation states of +4 and +6, and whereas both states have extremely rich coordination chemistry, they also differ greatly in preferred coordination environments.[21] Uranium(IV) is commonly eight- or nine-coordinate, although its coordination numbers can vary from 6 to 12, and the distribution of ligands in its coordination sphere is largely isotropic. However, when oxygen is present, uranium(VI) typically has two closely bonded oxygen atoms, which gives rise to the uranyl cation unit, UO_2^{2+}. Here, the coordination environment is generally limited to tetragonal, pentagonal, or hexagonal bipyramids, and its geometries are highly anisotropic because of the short, terminal oxo atoms. These fundamental differences lead to divergent extended structures, with U^{IV} usually yielding 3D networks, whereas U^{VI} is most often found in 2D sheets. Through the use of phosphite as a reducing ligand, there is also the possibility to make mixed-valent uranium compounds. Although mixed-valent uranium materials are known, they are not common.[22,23] There are also several reviews on the structural diversity within uranyl phosphate chemistry.[8h–j,21]

Herein, we will explore a second cesium carbonate/uranium/phosphite system. This system differs from the previous system as the concentration of the phosphite ligand has been lowered, and a completely new series of products are uncovered. The major influences on the products formed are the phosphite concentration, starting pH, and time. Here, we begin with a uranyl phosphate–phosphite or uranyl phosphite, expand through two intermediate phases, and then observe the two final U^{IV} phosphates. In this work, we are using the term "intermediate" to refer to the compounds that are forming in between the nonredox reacted product, U^{VI} phosphite, and the completely redox reacted product, U^{IV} phosphate, with the crystalline products observed, presumably, being the transitional compounds with the lowest solubilities. There is no implication of a solid-to-solid transformation, simply that the crystalline products isolated have either not completely reduced from U^{VI} to U^{IV} or not completely oxidized from P^{III} to P^{V}. The five new compounds described here illustrate the inherent complexity of the system and begin to illuminate the reaction pathways via the isolation of two intermediate disordered structures.

EXPERIMENTAL SECTION

Caution! *The $UO_2(NO_3)_2\cdot 6H_2O$ used in this study contained depleted uranium; standard precautions for handling radioactive materials, such as uranyl nitrate, should be followed.*

Syntheses. Uranyl nitrate $UO_2(NO_3)_2\cdot 6H_2O$ (International Bioanalytical Industries, Inc.), cesium carbonate (Alfa-Aesar, 99.9%), and phosphorous acid (Alfa-Aesar, 97%) were all used as received. All hydrothermal reactions were conducted in the same manner, unless otherwise listed. The reactants were mixed in their appropriate ratios and loaded into a 23 mL PTFE autoclave liner with 2 mL of distilled water. The liner was then sealed in a stainless steel autoclave and placed into a box furnace. The furnace was then ramped up to 200 °C for the desired number of hours (shown on the *x* axis of Figure 1) and then slowly cooled at a rate of 5 °C/h. Reactions were then washed with cold water, and the products were placed into a dish with ethanol for easier separation. Only compounds (**1**) and (**2**) could be made cleanly, with only (**2**) showing no impurities (see the Supporting Information). The impurity peaks shown in the Supporting Information in Figure 1.1.3 for (**1**) indicate another crystalline product; however, such a product was never visually found in the bulk sample for SC-XRD analysis. The authors, therefore, assume this to be a minor impurity. The peaks from the impurity do not easily match any of the other products or starting materials. The rest of the products listed below had to be individually picked out of the reaction mixtures (see the Supporting Information for crystal pictures). The reaction conditions listed below represent the amounts and reaction times for the specific crystals obtained for single-crystal diffraction; however, these compounds can be made at all of the conditions shown in Figure 1. Additionally, **0** was synthesized in our previous work and is shown in Figure 1 as it relates to the system.[20] Compounds were not placed back into the reaction vessel at the same reaction conditions, heated for longer, and again cooled to see if they would continue to convert, but has been shown to work previously,[20] likely through the product dissolving and continuing to react with the other reactants.

$Cs_4[(UO_2)_8(HPO_4)_5(HPO_3)_5]\cdot 4H_2O$ (1). Compound (**1**) was synthesized by combining 99.5 mg of uranyl nitrate (99 mM), 131.3 mg of Cs_2CO_3 (202 mM), and 167.0 mg of H_3PO_3 (1.019 M) into 2

dx.doi.org/10.1021/ic302198w | *Inorg. Chem.* 2013, 52, 965–973

Table 1. Crystallographic Data for All Listed Compounds: $Cs_4[(UO_2)_8(HPO_4)_5(HPO_3)_5]\cdot 4H_2O$ (1), $Cs[U^{IV}(PO_4)(H_{1.5}PO_4)]_2$ (2), $Cs_4[U^{IV}{}_6(PO_4)_8(HPO_4)(HPO_3)]$ (3), $Cs_{10}[U^{IV}{}_{10}(PO_4)_4(HPO_4)_{14}(HPO_3)_5]\cdot H_2O$ (4), and $Cs_3[U^{IV}{}_4(PO_4)_3(HPO_4)_5]$ (5)[c]

compound	1	2	3	4	5
mass	3629.61	988.85	2893.52	5829.71	2110.61
color and habit	light yellow, plate	forest green, plate	green, plate	dark green, plate	dark green, plate
space group	*C*2/*c* (No. 15)	*C*2/*c* (No. 15)	*Pmmn* (No. 59)	*C*2/*m* (No. 12)	*C*2/*c* (No. 15)
a (Å)	18.5005(7)	29.448(2)	6.9321(5)	19.2966(4)	18.018(2)
b (Å)	10.9710(4)	6.6314(3)	26.935(2)	20.2914(5)	9.2640(9)
c (Å)	14.4752(6)	6.9319(3)	10.9137(8)	13.9293(3)	17.516 (2)
α (deg)	90	90	90	90	90
β (deg)	104.513(3)	98.423(3)	90	126.839(1)	104.807(3)
γ (deg)	90	90	90	90	90
V (Å^3)	2844.2(2)	1339.0(1)	2037.8(3)	4365.0(2)	2826.7(5)
Z	2	4	2	2	4
T (K)	103(2)	100(2)	100(2)	100(2)	100(2)
ρ_{calcd} (g, cm^{-3})	4.238	4.905	4.716	4.435	4.959
μ(Mo Kα) (cmP^{-1P})	256.10	274.04	277.84	231.43	272.34
$R(F)$ for $F_o^2 > 2\sigma(FB_o^2)$P[a]	0.0465	0.0277	0.0377	0.0351	0.0284
$R_w(FB_o^2)$[b]	0.1010	0.0652	0.1003	0.0804	0.0661
goodness of fit on F^2	1.016	1.038	1.089	1.054	1.035

[a] $R(F) = \sum||F_o| - |F_c||/\sum|F_o|$. [b] $R_w(F_o^2) = [\sum[w(F_o^2 - F_c^2)^2]/\sum wF_o^4]^{1/2}$. [c] The numbered compounds relate to those found in Figure 1.

mL of distilled water. This yields an approximate ratio of reactants of $2Cs_2CO_3$:U^{VI}:$10H_3PO_3$. The liner was then sealed in a stainless steel autoclave, placed into a box furnace with the settings listed above, and heated at 200 °C for 2 h. A few of the light yellow plates were suitable for crystallographic studies and yielded the structure listed, yet many of the plates are heavily twinned with multiple domains. The approximate yields for syntheses of compound **1** range between 60% and 65%; however, the product likely contains a minor impurity (see the Supporting Information).

$Cs[U^{IV}(PO_4)(H_{1.5}PO_4)]_2$ (2). Compound (**2**) was synthesized by loading 99.6 mg of uranyl nitrate (99 mM), 131.2 mg of Cs_2CO_3 (201 mM), and 164.4 mg of H_3PO_3 (1.003 M) into a 23 mL PTFE autoclave liner with 2 mL of distilled water, which yields an approximate ratio of reactants of $2Cs_2CO_3$:U^{VI}:$10H_3PO_3$. The liner was then sealed in a stainless steel autoclave, placed into a box furnace with the settings listed above, and heated at 200 °C for 24 h. Several of the light green plates were suitable for crystallographic studies. The approximate yields for syntheses of compound **1** range between 75% and 85%; see the Supporting Information for PXRD on the bulk product.

$Cs_4[U^{IV}{}_6(PO_4)_8(HPO_4)(HPO_3)]$ (3). The first of the two U^{IV} compounds containing structural disorder was synthesized by loading 100.6 mg of uranyl nitrate (100 mM), 260.5 mg of Cs_2CO_3 (400 mM), and 165.5 mg of H_3PO_3 (1.009 M) into a 23 mL PTFE autoclave liner with 2 mL of distilled water, which yields an approximate ratio of reactants of $4Cs_2CO_3$:U^{VI}:$10H_3PO_3$. The liner was then sealed in a stainless steel autoclave, placed into a box furnace with the settings listed above, and heated at 200 °C for 72 h. Several of the leaf-shaped green plates (**3**) were suitable for crystallographic studies. Here, the *Z* was changed from 1 (calculated from checkcif) to 2, to yield the simplest formula.

$Cs_{10}[U^{IV}{}_{10}(PO_4)_4(HPO_4)_{14}(HPO_3)_5]\cdot H_2O$ (4). The second of the two U^{IV} compounds containing structural disorder was synthesized by loading 100.6 mg of uranyl nitrate (100 mM), 260.5 mg of Cs_2CO_3 (400 mM), and 165.5 mg of H_3PO_3 (1.009 M) into a 23 mL PTFE autoclave liner with 2 mL of distilled water. These amounts yield an approximate ratio of reactants of $4Cs_2CO_3$:U^{VI}:$10H_3PO_3$. The liner was then sealed in a stainless steel autoclave, placed into a box furnace with the settings listed above, and heated at 200 °C for 72 h. A few of the dark green block crystals (**4**) obtained were suitable for crystallographic studies. Along with both (**3**) and (**4**) forming at these conditions, there was also a hairlike product that formed with colors ranging from white to yellow to green. These were too small to diffract, could not be made pure, and were also not easily separated to get a clean sample for PXRD. Here, the *Z* was doubled from 1 (calculated from checkcif) to 2, to give the simplest formula.

$Cs_3[U^{IV}{}_4(PO_4)_3(HPO_4)_5]$ (5). Compound (**5**) was synthesized by loading 101.0 mg of uranyl nitrate (101 mM), 260.1 mg of Cs_2CO_3 (399 mM), and 164.8 mg of H_3PO_3 (1.005 M) into a 23 mL PTFE autoclave liner with 2 mL of distilled water, which yields an approximate ratio of reactants of $4Cs_2CO_3$:U^{VI}:$10H_3PO_3$. The liner was then sealed in a stainless steel autoclave, placed into a box furnace with the settings listed above, and heated at 200 °C for 96 h. Many of the dark green plates were suitable for crystallographic studies.

Crystallographic Studies. Crystals of all compounds were mounted on CryoLoops with Krytox oil and optically aligned on a Bruker APEXII Quazar X-ray diffractometer using a digital camera. Initial intensity measurements were performed using an IμS X-ray source and a 30 W microfocused sealed tube (Mo Kα, λ = 0.71073 Å) with high-brilliance and high-performance focusing Quazar multilayer optics. Standard APEXII software was used for determination of the unit cells and data collection control. The intensities of reflections of a sphere were collected by a combination of an appropriate number of exposures (frames). Each set had a different φ angle for the crystal, and each exposure covered a range of 0.5° in ω. SAINT software was used for data integration, including Lorentz and polarization corrections. Semiempirical absorption corrections were applied using the program SCALE (SADABS).[24] Crystallographic information for all obtained phases is summarized in Table 1. Atomic coordinates and additional structural information are provided in the Supporting Information (CIF).

Powder diffraction was collected on a Bruker D8 Advance with Davinci (Cu Kα, λ = 1.5405 Å) using a $\theta/2\theta$ geometry. The rotating sample was scanned from 5° to 90° 2Θ at a 0.02 increment and 13 s per step. Powder patterns were compared to calculated versions and can be found in the Supporting Information.

UV−vis-NIR Spectroscopy. UV−vis-NIR data were acquired from single crystals using a Craic Technologies microspectrophotometer. Crystals were placed on quartz slides under Krytox oil, and the data were collected from 200 to 1400 nm. The exposure time was auto-optimized by the Craic software. The characteristic peaks for the U^{6+} and U^{4+} are listed with the acquired spectra (see the Supporting Information).

SEM/EDS. Scanning electron microscope and energy-dispersive X-ray (SEM/EDS) analyses were collected on (**3**) and the unknown impurity that was found to form with the disordered compounds (**3**) and (**4**) using a LEO EVO 50 with an Oxford INCA energy dispersive spectrometer (see the Supporting Information). Samples were coated

dx.doi.org/10.1021/ic302198w | *Inorg. Chem.* 2013, 52, 965−973

with 2 nm of iridium. The energy of the electron beam was 29.02 kV. All of the data were calibrated with standards.

RESULTS AND DISCUSSION

In Figure 1, we present the evolution of products in a new cesium−uranium−phosphite system. This is similar to a previously presented system, but here, we have lowered the total phosphite concentration (where the ratio of H_3PO_3:UO_2^{2+} is 10:1) to explore how less of the reducing ligand will affect the products that form. The compounds are shown by number and relate to the products discussed above. Compound (**0**) is the only compound that was reported in our aforementioned work.[20] Previously, it was observed that the lower the cesium carbonate concentration, the more rapid the reduction of U^{VI} to U^{IV}. In this new system with lower phosphite concentrations, the reduction of uranium appears to be at a similar point for all cesium carbonate concentrations, but the oxidation of phosphite to phosphate observed in the crystalline phases is slowed at higher pHs. At lower cesium carbonate concentrations, there are only two products that form, beginning with an uranyl mixed phosphate−phosphate, which is followed by a simple U^{IV} phosphate. At higher cesium carbonate concentrations, we begin with a uranyl phosphite, followed by two intermediate U^{IV} compounds with ligand and/or cation disordering, and concluded with two different U^{IV} phosphate compounds. Herein, we will describe the system and the products formed within this new cesium−uranium−phosphite system.

Beginning at the lower cesium carbonate concentrations, and lower pH, the first product formed is that of a uranyl mixed phosphate−phosphite structure. Even with the reaction time held short, there is partial oxidation of the phosphite to phosphate while still keeping all of the uranium in its hexavalent form. $Cs_4[(UO_2)_8(HPO_4)_5(HPO_3)_5]\cdot 4H_2O$ (**1**) (shown in Figure 2) is obtained via a general reaction ratio of $2Cs_2CO_3$:U:$10H_3PO_3$. This uranyl mixed phosphate−phosphite yields an interesting (and thus far rare) topology observed only a few times before.[8g,25] The crystals of this 2D sheet are yellow plates, and the symmetry of this extended structure is *C*2/*c* (more information can be found in the Supporting Information). The repeating unit of three pentagonal bipyramids and one hexagonal bipyramid can be seen in Figure 2, bottom. This unit is surrounded by alternating phosphite and phosphate ligands, of which there are six of each. There is also some symmetry disordering associated with one of the phosphate ligands (P3) that is located on the top pentagonal bipyramid and the bottom of the hexagonal bipyramid.

Here, the pentagonal bipyramids have average uranyl oxygen bond lengths of 1.764(11) Å and the hexagonal bipyramids are nearly the same at 1.762(9) Å. The average U−O bonds in the equatorial plane for the pentagonal bipyramids are 2.377(9) Å. The average bond length for the equatorial oxygen atoms in the hexagonal bipyramids is longer at 2.453(7) Å. The bond valence sum (BVS) calculations for the three crystallographically unique U^{VI} sites yield values of 6.016, 6.258, and 6.130, respectively (see the Supporting Information for BVS calculations). The average P−O bond distance within the phosphite ligands is 1.496(9) Å, and the average P−O distance for the phosphate ligands is 1.559(10) Å. There is lengthening of the terminal phosphorus−oxygen bond distance for the protonated oxygen atoms on the phosphate ligands (see the Supporting Information). Crystals of this compound tend to be heavily twinned but form readily at lower pHs.

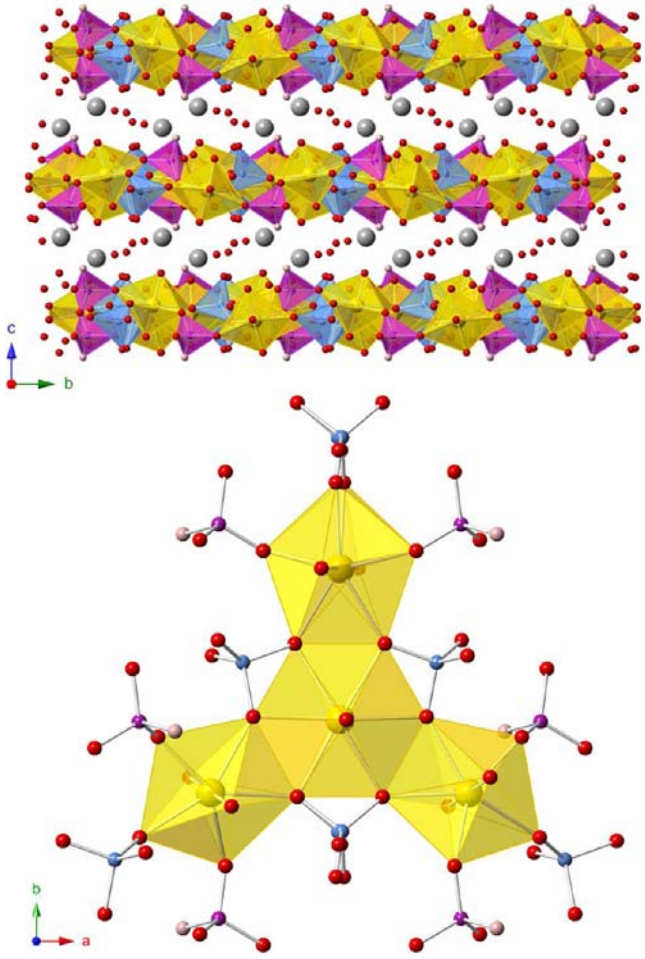

Figure 2. Top: The $Cs_4[(UO_2)_8(HPO_4)_5(HPO_3)_5]\cdot 4H_2O$ (**1**) sheet is shown in the [*bc*] plane, which crystallizes in the space group *C*2/*c*. Bottom: The building block of the sheet topology is made up of one hexagonal bipyramid and three pentagonal bipyramids, with alternating phosphate and phosphite ligand. In both figures, the uranyl units are yellow, phosphites are shown in purple, phosphates are shown in light blue, the oxygen atoms are red, and the hydrogen atoms are white.

If the reaction conditions are kept similar to (**1**), commonly $2Cs_2CO_3$:U:10 H_3PO_3, and the reaction is heated at 200 °C for at least 24 h, we observe complete reduction of U^{VI} to U^{IV} and oxidation of phosphite to phosphate. The reduced uranium(IV) phosphate formed is $Cs[U^{IV}(PO_4)(H_{1.5}PO_4)]_2$ (**2**) (Figure 3). This is the same structure type and topology as was previously found when Np^{VI} was hydrothermally reacted with phosphorous acid (both are *C*2/*c*).[19] The neptunium version was obtained by reacting Cs_2CO_3 with Np^{VI} and H_3PO_3 at a 1:2:10 ratio; with uranium, this product can also be obtained when using a lower ratio of U^{VI}:H_3PO_3 (1:10) and 1−2 equiv of Cs_2CO_3. A comparison of the two actinide(IV) phosphates is shown in Table 2. Here, the unit cell and average bond lengths for the uranium version are larger than that of the neptunium compound. Much like the previous neptunium phosphate, the crystals obtained for (**2**) are dark green plates, which look like elongated pentagons. At these low pH conditions, this product forms directly after compound (**1**) and is highly reproducible.

When looking at the one crystallographically unique uranium center, it is eight-coordinate with six corner-sharing and one edge-sharing phosphate ligand (Figure 3C). Like the Np^{IV}

dx.doi.org/10.1021/ic302198w | *Inorg. Chem.* 2013, 52, 965−973

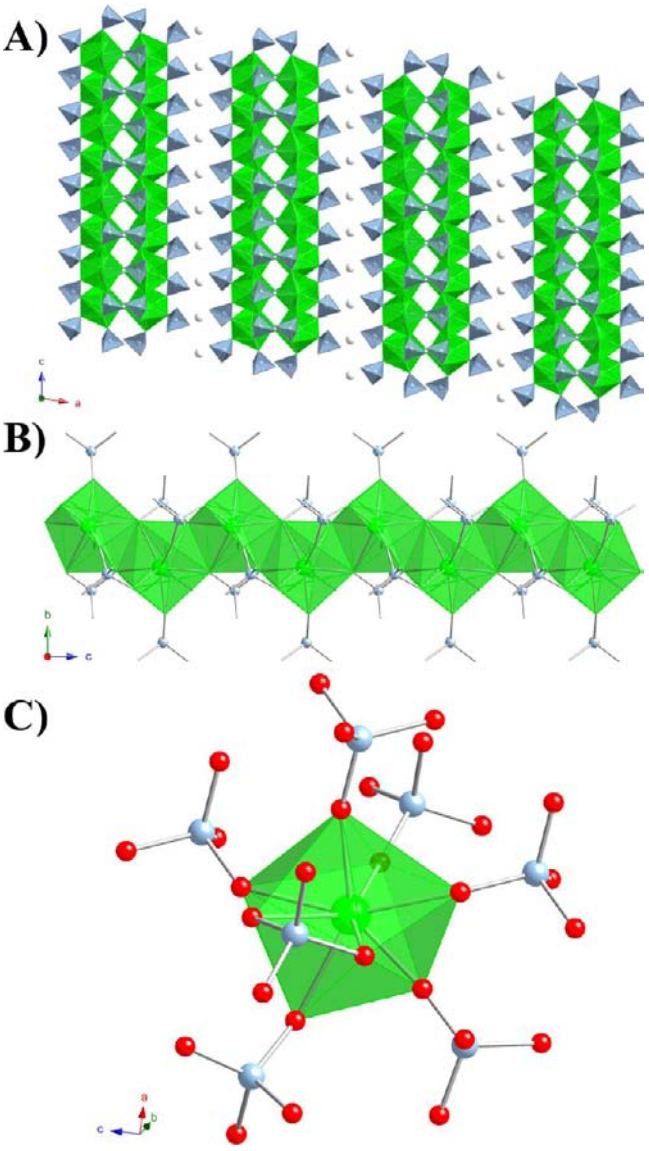

Figure 3. (A) The 2D sheet topology of $Cs[U^{IV}(PO_4)(H_{1.5}PO_4)]_2$ (**2**) as viewed in the [*ac*] plane; the cesium cations balance the charge between the sheets and crystallizes in the space group C2/*c*. (B) Here, an edge-sharing chain of U^{IV} is shown in the [*bc*] plane. These chains then link together, via the phosphates, to form the double uranium layer sheet topology shown in (A). (C) The eight-coordinate U^{IV} is shown here with five corner-sharing phosphates and one edge-sharing phosphate. In all, the uranium polyhedra are shown in green, phosphorus atoms (and phosphate tetrahedra) are in light blue, and the oxygen atoms are red (shown only in C for clarity).

version, in this cesium U^{IV} phosphate, the uranium center has an approximate local C_{2v} symmetry, which roughly yields a bicapped trigonal prismatic geometry, as determined by using the algorithm developed by Raymond and co-workers (see the Supporting Information).[26] The eight-coordinate U^{IV} polyhedra are then linked together via edge sharing and form an infinite 1D chain (Figure 3B). These chains connect together through phosphate polyhedra to form a double-layered uranium phosphate sheet (Figure 3A). Cesium cations are charge balancers in between these sheets. The $U^{IV}O_8$ polyhedra yield an average U−O bond length of 2.360(4) Å, whereas the P−O bond distances for the phosphate ligands are 1.536(5) Å. There is lengthening for the terminal, partially protonated oxygen atoms on half of the phosphate ligands (see the Supporting Information for BVS). Additionally, the BVS calculation for this U^{IV} site gives a slightly high value of 4.388 (see the Supporting Information).

If the same ratio of uranium to phosphorous acid is used as above (1:10), but more cesium carbonate is added in an effort to raise the pH, there is a large shift in the products that form. At short reaction times when using ratios higher than $2Cs_2CO_3$:U:$10H_3PO_3$, the previously made $Cs_2[(UO_2)_2(HPO_3)_3]\cdot H_2O$ (**0**) forms.[20] However, the crystals are much smaller than those found when higher phosphorous acid concentrations were used. When the reaction of $4Cs_2CO_3$:U:$10H_3PO_3$ is allowed to react for longer than 24 h at 200 °C, a few new phases are found in addition to a few crystals of (**0**). Two other compounds are formed in reasonable quantities, and both contain disorder of the cesium cations in the channels of these 3D networks. $Cs_4[U^{IV}_6(PO_4)_8(HPO_4)(HPO_3)]$ (**3**) is the first compound that is observed forming. These leaf-shaped crystals are light-green, are easily separated for single-crystal X-ray studies, and crystallize in the orthorhombic space group *Pmmn*. Figure 4 shows (**3**) as viewed in the [*bc*] plane; the cesium cations Cs3 and Cs4 reside in channels that run down the *a* axis. Two of the channels are roughly hexagonal and contain either two or three disordered cesium positions within them. The other channel is rectangular and contains three cesium positions (Cs2 cations). The Cs1 cations occupy a position that is close to the U4 and P5 sites. These atoms have 50% site occupancy and alternate within the statistic disorder.

There are four different U^{IV} positions in compound (**3**), three of which are seven-coordinate and one that is eight-coordinate (Figure 4, bottom). The average U^{IV}−O bond length for the first seven-coordinate uranium (U1) is 2.262(12) Å and contains six corner-sharing phosphate ligands and one corner-sharing phosphite ligand with an approximate mono-capped trigonal prism geometry. The second seven-coordinate uranium site (U2) is roughly a pentagonal bipyramid with five corner-sharing and one edge-sharing phosphate ligand and has an average U−O bond length of 2.304(9) Å. The third seven-coordinate uranium site (U3) has an average U−O bond length of 2.309(15) Å and six corner-sharing phosphate ligands and one corner-sharing phosphite. U3 also has a nearly pentagonal bipyramid geometry when one accounts for the symmetry disordering at the one phosphite ligand position. $U^{IV}O_8$ polyhedra for U4 has average U−O bond lengths of 2.412(13) Å and has six corner-sharing and one edge-sharing phosphate ligands. U4 has an approximate C_{2v} symmetry and a bicapped trigonal prism geometry (see the Supporting Information).[26] Additionally, U2 and U4 form an edge-sharing

Table 2. Comparison of the Two $Cs[An^{IV}(PO_4)(H_{1.5}PO_4)]_2$ Compounds, where An^{IV} is Np^{IV} or U^{IV}

An^{IV}-phosphate	average An^{IV}-O	*a*	*b*	*c*	volume
$Cs[U^{IV}(PO_4)(H_{1.5}PO_4)]_2$	2.372(4)	29.4481(14)	6.6314(3)	6.9319(3)	1339.07(11)
$Cs[Np^{IV}(PO_4)(H_{1.5}PO_4)]_2$	2.355(4)	29.449(4)	6.5800(8)	6.9092(9)	1323.4(3)

dx.doi.org/10.1021/ic302198w | *Inorg. Chem.* 2013, 52, 965−973

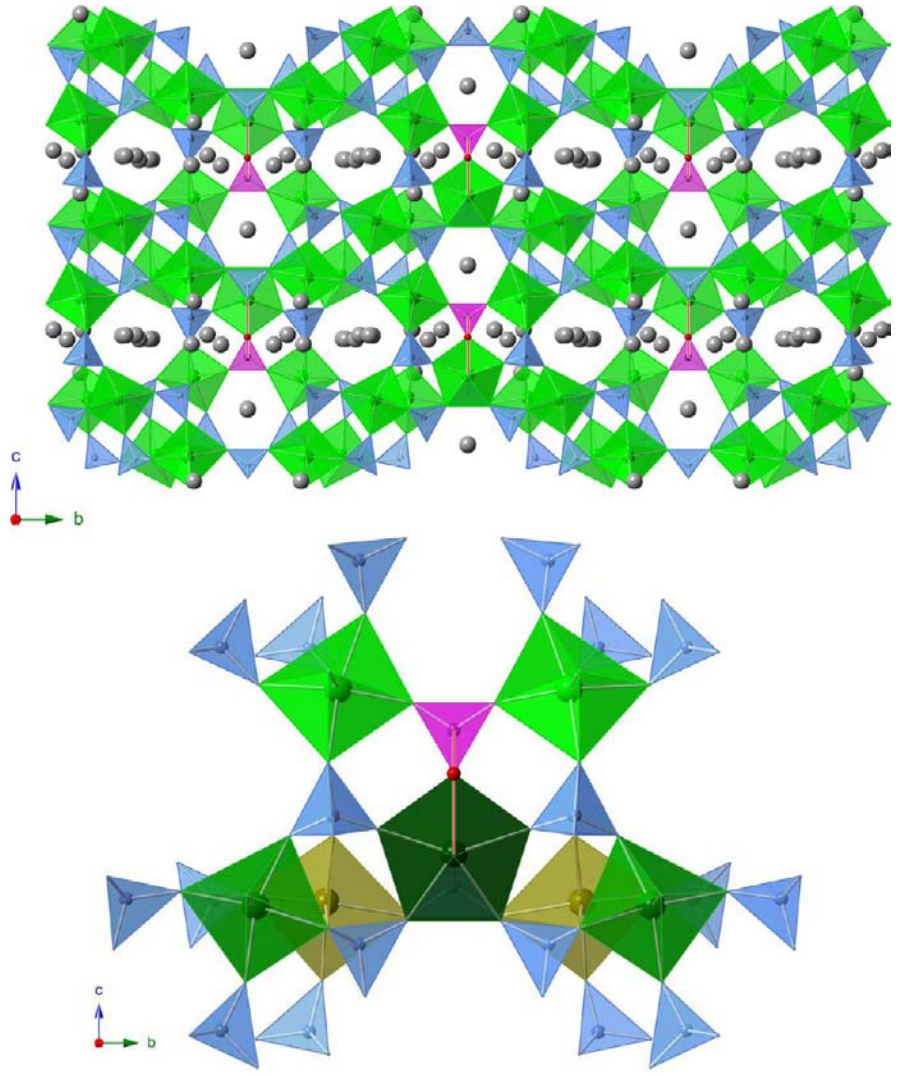

Figure 4. Top: The 3D network of $Cs_4[U^{IV}_6(PO_4)_8(HPO_4)(HPO_3)]$ (**3**) is shown down the *a* axis. This first of the two disordered compounds crystallizes in the orthorhombic space group *Pmmn*. Bottom: Here, the four different U^{IV} sites are shown in varying shades of green. The olive green (U4) uranium site is eight-coordinate, whereas the dark green (U3), the green (U2), and the light green (U1) uranium sites are seven-coordinate. In both top and bottom, the uranium polyhedra are shown in green, the phosphate tetrahedra are light blue, the phosphite tetrahedra are purple, and the cesium cations are shown in gray (omitted from the bottom for clarity).

chain that runs down the *a* axis. The BVS values for these U^{IV} sites are not ideal at 4.026, 4.336, 4.228, and 3.717, respectively; however, the UV−vis-NIR of the crystals clearly shows the presence of only uranium(IV) in the crystal (see the Supporting Information). In (**3**), there are mostly phosphate ligands, which have an average P−O bond length of 1.522(11) Å, with some lengthening for the terminally protonated oxygen atoms. The one phosphite ligand has a short average P−O bond length of 1.393(3) Å.

The second disordered phase that forms along with (**3**) is $Cs_{10}[U^{IV}_{10}(PO_4)_4(HPO_4)_{14}(HPO_3)_5]\cdot H_2O$ (**4**). Here, (**4**) contains not only cesium disordering but also phosphate−phosphite disordering at several of the ligand positions. These blocky crystals are easily picked out as they are drastically different from (**3**) and crystallize in the monoclinic space group *C*2/*m*; see the Supporting Information for crystal pictures. The three-dimensional network can be seen in Figure 5A as viewed in the [*bc*] plane showing the layers of U^{IV} and in the [*ac*] plane (Figure 5B) illustrating the channels in the network. There are three different uranium sites forming trimers (Figure 5C) and dimers (Figure 5D), which are linked together via both phosphate and phosphite ligands resulting in 2D layers. These layers are connected by disordered PO_4 and HPO_3 groups into a 3D framework. There are three disordered cesium positions (Cs2−Cs4) that reside within the complex system of channels. The Cs1 position is not disordered. SEM/EDS analysis was conducted on the disordered compound (**3**) to make sure there were no other cations in the crystal; only cesium, uranium, and phosphorus were found (see the Supporting Information).

In (**4**), there are three different U^{IV} centers, two of which are eight-coordinate and one that is nine-coordinate. The average U−O bond length for the nine-coordinate uranium (U1) is 2.431(7) Å and contains one corner-sharing phosphite, four corner-sharing phosphates, and two edge-sharing phosphate ligands, which form an approximate monocapped square antiprism geometry (Figure 5C; dark green polyhedra). The first of the eight-coordinate uranium centers (U2) has six corner-sharing and one edge-sharing phosphate ligand and an estimated D_{2d} symmetry with a trigonal dodecahedron geometry.[26] Here, the average U−O bond length in U2 is

dx.doi.org/10.1021/ic302198w | *Inorg. Chem.* 2013, 52, 965−973

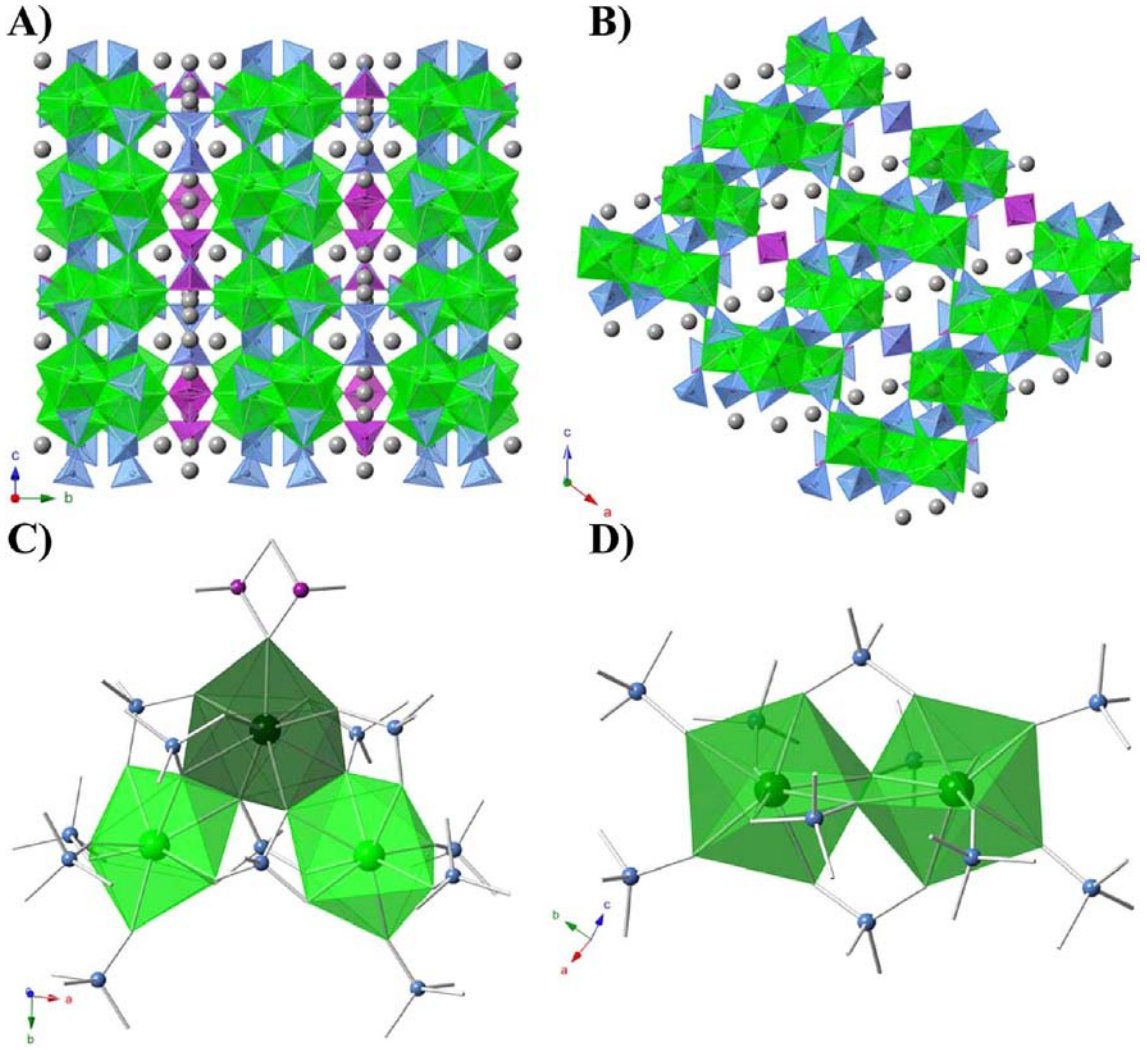

Figure 5. (A) Here, the second of the two disordered compounds $Cs_{10}[U^{IV}{}_{10}(PO_4)_4(HPO_4)_{14}(HPO_3)_5]\cdot H_2O$ (**4**), which crystallizes in the space group $C2/m$, is displayed in the $[bc]$ plane showing the phosphate and phosphite ligands that link the layers of U^{IV} together (B) Here, the 3D network of (**4**) is shown in the $[ac]$ plane to illustrate the small channels that run down the b axis. The three uranium centers are shown as an edge-sharing trimer of U1 and U3 (**C**) and as an edge-sharing dimer of U2 (**D**) in varying shades of green. Here, the dark green center (U1) is nine-coordinate and the two lighter green centers (U2 and U3) are eight. The uranium polyhedra are in green, phosphates are in light blue, the phosphites are in purple, and charge balancing cesium cations are shown in light gray (top only), with the phosphate−phosphite disordering removed for clarity.

2.367(7) Å. This U2 site is also edge-sharing with itself to form a U^{IV} dimer (Figure 5D). The second eight-coordinate site (U3) has also has six corner-sharing and one edge-sharing phosphate ligand with an average U−O bond length of 2.365(7) Å but has roughly C_{2v} symmetry, which gives a bicapped trigonal prism geometry (Figure 5C; light green).[26] Combined with U1, two U3 sites help to form a U^{IV} trimer with the U1 site in the middle of the two U3 (Figure 5C). The BVS values for these three sites are 3.840, 4.121, and 4.190, for U1, U2, and U3, respectively. The phosphate ligands show an average P−O bond distance of 1.527(12) Å, with some lengthening for the protonated oxygen atoms on the HPO_4^{2-} units. The average P−O bond length for the phosphite ligands is very similar at 1.502(19) Å. The high error on these bond lengths is caused by the phosphate−phosphite disordering that is observed on three of the ligand positions.

In addition to (**3**) and (**4**) forming, there is another product that is found in these reaction products. It is at least one (if not two or more) microcrystalline powder(s) that have not yet been successfully structurally determined. Thus far, it has been quite difficult to cleanly separate these out for more characterization techniques as there are several colors in the hairlike crystals and the crystals of (**0**), (**3**), (**4**), and (**5**) tend to be interwoven within this product. SEM/EDS was conducted on the impurity with cesium, uranium, and phosphorus being the dominant species (see the Supporting Information). There was a minor nickel impurity; however, it has a very low abundance. No nickel was ever used in these syntheses and, as such, may or may not be an actual impurity. Further attempts have been made to obtain a pure phase but have thus far been unsuccessful. This product eventually does stop forming as the reaction time is extended out further.

Looking back at Figure 1, if the reaction of $4Cs_2CO_3$:U:$10H_3PO_3$ is allowed to react for 96 h at 200 °C, a new, nondisordered phase begins to form. The final new compound in this series forms dark green plates that crystallize in the monoclinic space group $C2/c$. Figure 6 (top) shows the 3D phase of $Cs_3[U^{IV}{}_4(PO_4)_3(HPO_4)_5]$ (**5**) as viewed down the b axis. Here, the cesium atoms are balancing the charge in the channels and there is no disordering of the cations. The

dx.doi.org/10.1021/ic302198w | *Inorg. Chem.* 2013, 52, 965−973

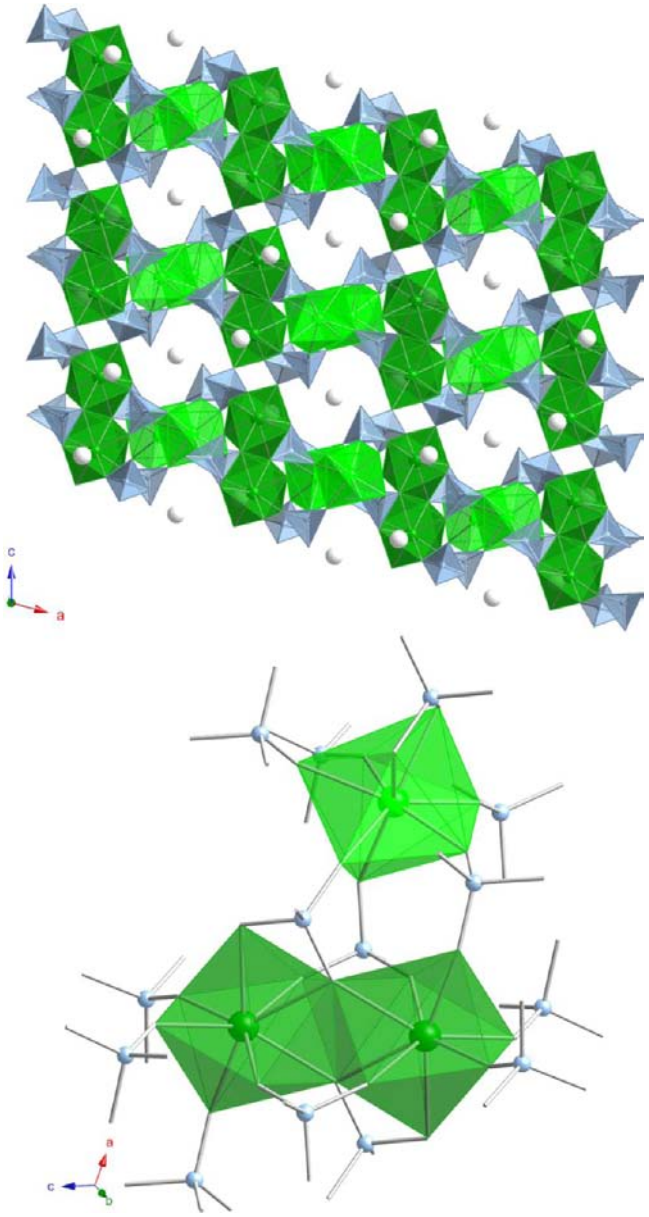

Figure 6. Top: The final structure in the series is a 3D network of U^{IV} and phosphate shown in the [*ac*] plane, which yields $Cs_3[U^{IV}_4(PO_4)_3(HPO_4)_5]$ (**5**) and crystallizes in the space group *C*2/*c*. Here, the nondisordered cesium cations balance the charge in the channels, which run down the *b* axis. Bottom: There are two different U^{IV} centers, and both are eight-coordinate, with the dark green centers forming an edge-sharing dimer. The uranium polyhedra are in green, phosphates are in light blue, cesium cations are dark gray (top only), and oxygen are omitted for clarity.

transition has been made through the disordered cesium and disordered P^{5+}/P^{3+} intermediates (compounds **3** and **4**) to the more robust U^{IV} phosphate. It is also clear that all the phosphite has finally reacted away and that there is only the now oxidized phosphate to react with the reduced U^{IV}.

There are two unique U^{IV} sites, one that forms an edge-sharing dimer and the other is coordinated to just phosphate ligands (Figure 6, bottom). The latter site (U2) is eight-coordinate and has six corner-sharing phosphates and one edge-sharing phosphate. U2 has an average U−O bond length of 2.373(4) Å and exhibits a nearly D_{4d} symmetry and a square antiprism geometry.[26] The other uranium site (U1) is also eight-coordinate and forms a U^{IV} edge-sharing dimer. The average U−O bond length for U1 is 2.372(4) Å, and like U2, it also has six corner-sharing and an edge-sharing phosphate ligand. However, the U1 is a lower approximate symmetry at D_{2d}, yielding a trigonal dodecahedron.[26] The BVS value for U1 is 4.061 and is 4.095 for U2, a much better fit than the values that were calculated for the two disordered structures. Here, the average phosphate P−O bond distance is 1.537(5) Å and the average bond length for the protonated P−O units is longer at 1.588(6) Å. In an attempt to purify the synthesis of (**5**), the reaction time was extended out to 7 days; however, compound (**2**) began to form in addition instead. Thus far, these two are the final products that have been obtained for these longer reactions.

CONCLUSION

Through utilization of hydrothermal syntheses involving in situ redox reactions, we were able to elucidate the complex chemistry of this new system. Like in our previous work,[20] the evolution of products in this cesium−uranium−phosphite series appears to be strongly dependent on time and on the cesium carbonate concentration, which affects the starting pH of the reaction mixture. The redox chemistry is slowed with increasing cesium carbonate concentrations. However, instead of mixed-valent uranium compounds as intermediates, the transitional structures above, (**3**) and (**4**), contained substantial amounts of cation disordering, the latter of which also contains disordered phosphate−phosphite ligands. With a ratio of reactants of $4Cs_2CO_3$:UO_2^{2+}:$10H_3PO_3$ (Figure 1), the system begins with a simple uranyl phosphite, transitions through two disordered intermediate structures, and ends with two U^{IV} phosphate compounds. Presumably, the disordered crystalline products observed are the redox intermediate phases with the lowest solubilities. Therefore, while the title compounds help to illuminate the complexities of these hydrothermal redox reactions, they also serve as a route to producing new stable and insoluble extended networks of uranium(IV) phosphate.

ASSOCIATED CONTENT

Supporting Information

Bond lengths and UV−vis-NIR, crystal pictures, powder diffraction data, and bond valence sum calculations for all of the compounds listed. This material is available free of charge via the Internet at http://pubs.acs.org.

AUTHOR INFORMATION

Corresponding Author

*E-mail: e.alekseev@fz-juelich.de (E.V.A.), talbrechtschmitt@gmail.com (T.E.A.-S.).

Notes

The authors declare no competing financial interest.

ACKNOWLEDGMENTS

We are grateful for support provided as part of the Materials Science of Actinides, an Energy Frontier Research Center funded by the U.S. Department of Energy, Office of Science, Office of Basic Energy Sciences, under Award Number DE-SC0001089. We would also like to thank the Center for Sustainable Energy at Notre Dame for the use of their instrumentation. E.V.A. was supported by the VH-NG-815 grant of the Helmholtz Association.

REFERENCES

(1) Tabuteau, A.; Pages, M.; Livet, J.; Musikas, C. J. *Mater. Sci. Lett.* **1988**, *7*, 1315.
(2) Begg, B. D.; Vance, E. R.; Conradson, S. D. *J. Alloys Compd.* **1998**, *271*, 221.
(3) Dacheux, N.; Thomas, A. C.; Chassigneux, B.; Pichot, E.; Brandel, V.; Genet, M. *Mater. Res. Soc. Symp. Proc.* **1999**, *556*, 85.
(4) Dacheux, N.; Thomas, A. C.; Chassigneux, B.; Pichot, E.; Brandel, V.; Genet, M. *Ceram. Trans.* **1999**, *93*, 373.
(5) Kitaev, D. B.; Volkov, Y. F.; Orlova, A. I. *Radiochemistry.* **2004**, *46*, 211.
(6) Volkov, Y. F.; Tomilin, S. V.; Orlova, A. I.; Lizin, A. A.; Spiryakov, V. I.; Lukinykh, A. N. *Russ. J. Inorg. Chem.* **2005**, *50*, 1660.
(7) Wellman, D. M.; Mattigod, S. V.; Parker, K. E.; Heald, S. M.; Wang, C.; Fryxell, G. E. *Inorg. Chem.* **2006**, *45*, 2382.
(8) (a) Bray, T. H.; Nelson, A. G. D.; Jin, G. B.; Haire, R. G.; Albrecht-Schmitt, T. E. *Inorg. Chem.* **2007**, *46*, 10959. (b) Nelson, A. G. D.; Bray, T. H.; Zhan, W.; Haire, R. G.; Sayler, T. S.; Albrecht-Schmitt, T. E. *Inorg. Chem.* **2008**, *47*, 4945. (c) Nelson, A. G. D.; Bray, T. H.; Albrecht-Schmitt, T. E. *Angew. Chem., Int. Ed.* **2008**, *47*, 6252. (d) Nelson, A. G. D.; Bray, T. H.; Stanley, F. A.; Albrecht-Schmitt, T. E. *Inorg. Chem.* **2009**, *48*, 4530. (e) Diwu, J.; Nelson, A. G. D.; Albrecht-Schmitt, T. E. *Comments Inorg. Chem.* **2010**, *31*, 46. (f) Diwu, J. A.; Wang, S. A.; Liao, Z.; Burns, P. C.; Albrecht-Schmitt, T. E. *Inorg. Chem.* **2010**, *49*, 10074. (g) Diwu, J.; Wang, S.; Good, J. J.; DiStefano, V. H.; Albrecht-Schmitt, T. E. *Inorg. Chem.* **2011**, *50*, 4842. (h) Diwu, J.; Albrecht-Schmitt, T. E. In *Metal Phosphonate Chemistry: From Synthesis to Applications*; Clearfield, A., Demadis, K., Eds.; The Royal Society of Chemistry: London, 2012. (i) Knope, K. E.; Cahill, C. L. In *Metal Phosphonate Chemistry: From Synthesis to Applications*; Clearfield, A., Demadis, K., Eds.; The Royal Society of Chemistry: London, 2012. (j) Andrews, M. B.; Cahill, C. L. *Chem. Rev.* 2012. DOI: 10.1021/cr300202a.
(9) (a) Koskenlinna, M.; Valkonen, J. *Acta Crystallogr.* **1996**, *C52*, 1857. (b) Cooper, M. A.; Hawthorne, F. C. *Can. Mineral.* **2001**, *39*, 797. (c) Almond, P. M.; Peper, S. M.; Bakker, E.; Albrecht-Schmitt, T. E. *J. Solid State Chem.* **2002**, *168*, 358. (d) Sullens, T. A.; Almond, P. M.; Byrd, J. A.; Beitz, J. V.; Bray, T. H.; Albrecht-Schmitt, T. E. *J. Solid State Chem.* **2006**, *179*, 1192. (e) Bray, T. H.; Skanthakumar, S.; Soderholm, L.; Sykora, R. E.; Haire, R. G.; Albrecht-Schmitt, T. E. *J. Solid State Chem.* **2008**, *181*, 493.
(10) (a) Brandstätter, F. *Z. Kristallogr.* **1981**, *155*, 193. (b) Namboodiri, P. N.; Tripathi, S. N. *J. Mater. Sci.* **2000**, *35*, 337. (c) Almond, P. M.; Albrecht-Schmitt, T. E. *Inorg. Chem.* **2002**, *41*, 5495. (d) Woodward, J. D.; Albrecht-Schmitt, T. E. *J. Solid State Chem.* **2005**, *178*, 2922. (e) Ling, J.; Ward, M.; Burns, P. C. *J. Solid State Chem.* **2011**, *184*, 401.
(11) (a) Tsivadze, A. Y.; Krot, N. N.; Muchnik, B. I. *Proc. Moscow Symp. Chem. Transuranium Elem.* **1976**, 89. (b) Bean, A. C.; Ruf, M.; Albrecht-Schmitt, T. E. *Inorg. Chem.* **2001**, *40*, 3959. (c) Sykora, R. E.; McDaniel, S. M.; Wells, D. M.; Albrecht-Schmitt, T. E. *Inorg. Chem.* **2002**, *41*, 5126. (d) Bray, T. H.; Ling, J.; Choi, E. S.; Brooks, J. S.; Beitz, J. V.; Sykora, R. E.; Haire, R. G.; Stanbury, D. M.; Albrecht-Schmitt, T. E. *Inorg. Chem.* **2007**, *46*, 3663.
(12) Chretien, A.; Kraft, J. C.; Hebd, R. *C. R. Seances Acad. Sci.* **1937**, *204*, 1936.
(13) Avduevskaya, K. A.; Rozanov, I. A.; Mironova, V. S. *Inorg. Mater.* **1977**, *13*, 1515.
(14) Avduevskaya, K. A.; Ragulina, N. B.; Rozanov, I. A. *Inorg. Mater.* **1981**, *17*, 834.
(15) Mistryukov, V. E.; Mikhailov, Y. N. *Koord. Khim.* **1985**, *11*, 1393.
(16) Doran, M.; Walker, S. M.; O'Hare, D. *Chem. Commun.* **2001**, 1988.
(17) Xu, J. F.; Li, H. H.; Cao, Y. N.; Huang, C. C.; Zhang, H. H.; Lin, D. S.; Yang, Q. Y.; Sun, R. Q. *Chin. J. Struct. Chem.* **2006**, *25*, 1380.
(18) Mandal, S.; Chandra, M.; Natarajan, S. *Inorg. Chem.* **2007**, *46*, 7935.
(19) (a) Villa, E. M.; Wang, S.; Alekseev, E. V.; Depmeier, W.; Albrecht-Schmitt, T. E. *Eur. J. Inorg. Chem.* **2011**, 3749. (b) Cross, J. N.; Villa, E. M.; Wang, S.; Diwu, J.; Polinski, M. J.; Albrecht-Schmitt, T. E. *Inorg. Chem.* **2012**, *51*, 8419.
(20) (a) Villa, E. M.; Marr, C. J.; Jouffret, L. J.; Alekseev, E. V.; Depmeier, W.; Albrecht-Schmitt, T. E. *Inorg. Chem.* **2012**, *51*, 6548. (b) Compound was incorrectly listed in the original manuscript as $Cs_2[(UO_2)_2(HPO_3)_3(H_2O)]$ and should have been written correctly, as in the CIF, as $Cs_2[(UO_2)_2(HPO_3)_3]\cdot H_2O$.
(21) (a) Burns, P. C.; Miller, M. L.; Ewing, R. C. *Can. Mineral.* **1996**, *34*, 845. (b) Burns, P. C.; Ewing, R. C.; Hawthorne, F. C. *Can. Mineral.* **1997**, *35*, 1551. (c) Burns, P. C. In *Uranium: Mineralogy, Geochemistry and the Environment*; Burns, P. C., Finch, R., Eds.; Mineralogical Society of America: Washington, DC, 1999; Chapter 1. (d) Burns, P. C. *Mater. Res. Soc. Symp. Proc.* **2004**, *802*, 89. (e) Burns, P. C. *Can. Mineral* **2005**, *43*, 1839. (f) Burns, P. C. In *Structural Chemistry of Inorganic Actinide Compounds*; Krivovichev, S. V., Burns, P. C., Tananaev, I. G., Eds.; Elsevier: Amsterdam, The Netherlands, 2007; Chapter 1.
(22) (a) Kepert, D. L.; Patrick, J. M.; White, A. H. *J. Chem. Soc., Dalton Trans.* **1983**, 381. (b) Bombieri, G.; Benetollo, F.; Klahne, E.; Fischer, D. *J. Chem. Soc., Dalton Trans.* **1983**, 1115. (c) Benard, P.; Louer, D.; Dacheux, N.; Brandel, V.; Genet., M. *Chem. Mater.* **1994**, *6*, 1049. (d) Allen, S.; Barlow, S.; Halasyamani, P.; Mosselmans, J.; O'Hare, D.; Walker, S. M.; Walton, R. I. *Inorg. Chem.* **2000**, *39*, 3791. (e) Wang, C. M.; Liao, C. H.; Lin, H. M.; Lii, K. H. *Inorg. Chem.* **2004**, *43*, 8239. (f) Berthet, J. C.; Thuery, P.; Dognon, J. P.; Guillaneux, D.; Ephritikhine, M. *Inorg. Chem.* **2008**, *47*, 6850. (g) Lin, C. H.; Lii, K. H. *Angew. Chem.* **2008**, *120*, 8839. (h) Mougel, V.; Horeglad, P.; Nocton, G.; Pecaut, J.; Mazzanti, M. *Angew. Chem., Int. Ed.* **2009**, *48*, 8477. (i) Andreev, G.; Budantseva, N.; Tananaev, I.; Myasoedov, B. *Inorg. Chem. Commun.* **2010**, *13*, 577. (j) Nguyen, Q. B.; Liu, H. K.; Chang, W. J.; Lii, K. H. *Inorg. Chem.* **2010**, *50*, 4241.
(23) (a) Burns, P. C.; Finch, R. J.; Hawthorne, F. C.; Miller, M. L.; Ewing, R. C. *J. Nucl. Mater.* **1997**, *249*, 199. (b) Burns, P. C.; Finch, R. J. *Am. Mineral.* **1999**, *84*, 1456. (c) Belai, N.; Frisch, M.; Liton, E.; Ravel, B.; Cahill, C. L. *Inorg. Chem.* **2008**, *47*, 10135.
(24) (a) Sheldrick, G. M. *SADABS: Program for Absorption Correction Using SMART CCD* (based on the method of Blessing); University of Göttingen: Göttingen, Germany. (b) Blessing, R. H. *Acta Crystallogr.* **1995**, *A51*, 33.
(25) Wylie, E. M.; Burns, P. C. *Can. Mineral.* **2012**, *50*, 147.
(26) (a) Kepert, D. L. *Prog. Inorg. Chem.* **1978**, *24*, 179. (b) Xu, J.; Radkov, E.; Ziegler, M.; Raymond, K. N. *Inorg. Chem.* **2000**, *39*, 4156. (c) Gorden, A. V.; Xu, J.; Raymond, K. N.; Durbin, P. *Chem. Rev.* **2003**, *103*, 4207.